



Available online at www.sciencedirect.com

ScienceDirect

journal homepage: <http://www.elsevier.com/locate/rpor>



Original research article

Validation of dose distribution computation on sCT images generated from MRI scans by Philips MRCAT



Iva Bratova*, Petr Paluska, Jakub Grepl, Petra Sykorova, Jan Jansa, Miroslav Hodek, Igor Sirak, Milan Vosmik, Jiri Petera

Department of Oncology and Radiotherapy, University Hospital Hradec Kralove, Czech Republic

ARTICLE INFO

Article history:

Received 14 September 2018

Received in revised form

26 November 2018

Accepted 7 February 2019

Available online 28 February 2019

Keywords:

MRCAT

Prostate cancer

sCT

Radiotherapy

ABSTRACT

Aim: To evaluate calculation of treatment plans based on synthetic-CT (sCT) images generated from MRI.

Background: Because of better soft tissue contrast, MR images are used in addition to CT images for radiotherapy planning. However, registration of CT and MR images or repositioning between scanning sessions introduce systematic errors, hence suggestions for MRI-only therapy. The lack of information on electron density necessary for dose calculation leads to sCT (synthetic CT) generation. This work presents a comparison of dose distribution calculated on standard CT and sCT.

Materials and methods: 10 prostate patients were included in this study. CT and MR images were collected for each patient and then water equivalent (WE) and MRCAT images were generated. The radiation plans were optimized on CT and then recalculated on MRCAT and WE data. 2D gamma analysis was also performed.

Results: The mean differences in the majority of investigated DVH points were in order of 1% up to 10%, including both MRCAT and WE dose distributions. Mean gamma pass for acceptance criteria 1%/1 mm were greater than 82.5%. Prescribed doses for target volumes and acceptable doses for organs at risk were met in almost all cases.

Conclusions: The dose calculation accuracy on MRCAT was not significantly compromised in the majority of clinical relevant DVH points. The introduction of MRCAT into practise would eliminate systematic errors, increase patients' comfort and reduce treatment expenses. Institutions interested in MRCAT commissioning must, however, consider changes to established workflow.

© 2019 Greater Poland Cancer Centre. Published by Elsevier B.V. All rights reserved.

* Corresponding author at: Department of Oncology and Radiotherapy, University Hospital, Sokolska 581, Hradec Kralove 500 05, Czech Republic.

E-mail address: iva.bratova@gmail.com (I. Bratova).

<https://doi.org/10.1016/j.rpor.2019.02.001>

1507-1367/© 2019 Greater Poland Cancer Centre. Published by Elsevier B.V. All rights reserved.

1. Background

Computed tomography (CT) is a standard method used for radiotherapy planning. However, this modality provides only a little soft tissue resolution, hence complementary use of magnetic resonance imaging (MRI) which is suitable for precise delineation of target volumes in soft tissue. Since MRI does not provide attenuation information, registration of CT and MRI images is necessary. This approach may be a source of many systematic errors including set-up and positioning differences between imaging sessions or those originating from image registration in the planning system.¹ Various authors^{2,3} have reported systematic registration errors for prostate from 0.5 to 3 mm (strongly dependent on registration method). In order to improve medical care, some alternative methods have been proposed.

One of these alternatives to the standard CT-based planning is the MRI-only approach. The main idea is to generate synthetic CT (sCT) from MRI images, where Hounsfield units (HU) are assigned to respective body regions using only MRI information. The biggest asset of one-modality approach is reduction of systematic errors described above. Moreover, the planning process itself can be reduced resulting in lower treatment expenses. On the other hand, MRI-only methods face other restrictions connected with sCT generation and the principle of MRI itself.⁴ These aspects will be further discussed.

Methods of generating sCT images may be categorized into three classes: (1) atlas-based, (2) voxel-based, (3) bulk assignment-based techniques,¹ supplemented by hybrid techniques. The basic idea of atlas-based methods is to create a database of CT and MRI images. Then, a single MRI image of a patient is typically sufficient for sCT generation.⁵ Results on this topic were presented by various authors.⁶ Voxel-based methods involve several standard or specialized sequences. Their specific properties enable to create the resulting density map.

Bulk-assignment methods separate the tissues in MRI image into several classes and each one is assigned an electron density or HU. The simplest method of sCT generation from an MRI is to assign one electron density to the whole patient volume, usually water equivalent. More sophisticated methods were also introduced.⁷ Nevertheless, the number of various approaches have been presented so far, some of which have applied advanced computational methods^{8,9} that cannot be simply categorized as described above. Generally, each of these methods has its advantages and limitations regarding the number of tissue classes, atypical anatomy, etc. The main sites tested are the prostate, brain, head and neck⁴ but other sites deserve attention as well and should be the focus of future research.

In this work, commercial system MRCAT (Magnetic Resonance for Calculating Attenuation) by Philips was applied. MRCAT is an automatic system using several MRI sequences to create sCT and operating with 5 values of HU, that is 5 categories of tissues (air, compact and spongy bone, fat, water-rich tissue).¹⁰ MRCAT is so far available only for the pelvis region,

thus only prostate patients were investigated. A comparison of MRI, CT and MRCAT images can be seen in Fig. 1.

2. Aim

The aim of this study was to evaluate radiation plans based on sCT images generated by MRCAT. Assets and shortcomings of MRCAT are also discussed.

3. Materials and methods

3.1. Patients characteristics

Plans of ten prostate cancer patients were evaluated in this planning study. Patients were treated using intensity modulated radiotherapy (IMRT) to prostate with simultaneous integrated boost (SIB) to the proximal part of the seminal vesicles. All of them underwent standard CT simulation and MRI.

3.2. Dose calculation

A Siemens Somatom Sensation Open (Siemens Medical Solutions) was used for CT image acquisition. Image was reconstructed with 2.5 mm slice thickness, 512 × 512 matrix, pixel size 0.98 mm. MRCAT images were generated from MRI images acquired on Philips Ingenia 1.5T (Philips Healthcare) with slice thickness 2.5 mm. All images were imported to the treatment planning system EclipseTM, version 13.5 (Varian Medical Systems).

In order to keep patients' position reproducible, they were scanned and irradiated in the treatment position, i.e. in a supine position with Dual Leg Positioner (Civco Medical Solutions) to immobilize their legs and pelvis. Patients were also asked to follow some specific instructions to avoid a markedly different rectum and bladder filling between sessions. They were instructed to empty their rectum before planning CT acquisition and before each irradiation session. Application of suppositories was recommended in case the rectum volume exceeded 120 cm³ at the planning CT and the scanning was repeated afterwards. Their bladders should be slightly filled which can be achieved by drinking 500 ml of water before image acquisition.

All involved patients were scanned on MRI and immediately after that on CT, usually within 10 min. The images were transferred to the EclipseTM system and image registration was performed. Referring to Philips official recommendation,¹¹ the type of registration should be taken into consideration. For CT and MRCAT registration, we carried out rigid registration using translation of images. Ghilezan et al.¹² states that a prostate displacement of ≤3 mm can be expected for 20 min following the moment of initial imaging for patients with an empty rectum. These conditions were met as described above. In addition, the prostate contour cannot be accurately detected on the CT, so the accuracy of the registration is implicitly limited. For these reasons, we consider the chosen registration method as sufficient. Nevertheless, in case the time span between the MRI and CT acquisition is



Fig. 1 – Comparison of MRI (left), CT (middle) and MRCAT (right) images. MRI image is presented by T2w scan.

Table 1 – Prescription doses for planning target volumes and acceptable doses for organs at risk.

Structure	Prescription
Prostate (PTV2)	Prescribed dose 78 Gy = mean dose for PTV2. Minimally 95% of the prescribed dose (i.e. 74.1 Gy) to 95% of the PTV2. Maximal dose \leq 107% of the prescribed dose (i.e. 83.5 Gy).
Seminal vesicles (PTV1–2)	Prescribed dose 72.15 Gy. Minimally 95% of the prescribed dose (i.e. 68.5 Gy) to 95% of the PTV1–2. Maximal dose \leq 107% of the prescribed dose (i.e. 77.2 Gy).
Rectum	Maximally 50% can receive 50 Gy. Maximally 25% can receive 70 Gy. Maximally 15% can receive 75 Gy and maximally 15 cm ³ can receive 75 Gy. Maximum dose 78 Gy.
Bladder	Maximally 30% can receive 70 Gy. Maximally 15% can receive 75 Gy and maximally 15 cm ³ can receive 75 Gy. Maximum dose 78 Gy.

more prominent, it may be necessary to consider more sophisticated registration methods.¹³

Target volumes were delineated on CT with respect to MRI. Clinical target volumes (CTVs) were delineated as follows: CTV1 represents prostate and the proximal part of the seminal vesicles, CTV2 only prostate. Planning target volumes (PTVs) were delineated like this: PTV1 was obtained by application of a 7 mm margin to CTV1 in all directions. PTV2 was defined in the same manner. PTV1–2 was formally defined by subtraction PTV1–PTV2. Organs at risk (OARs) are the whole rectum and bladder. Dose to other anatomical sites, as the penile bulb or femoral heads, are insignificant and, therefore, not included in our clinical standard.

Five 6 MV photon fields were used to deliver total dose of 78 Gy for PTV2 and 72.15 Gy for PTV1–2 in 39 fractions. Criteria for optimization are presented in Table 1. Standard plans based on CT data (hereafter CT plans) were created. Subsequently, plans were transferred to MRCAT images without any changes in plan origin, MU, field positions, etc. Plans were recalculated without optimization.

3.3. Dosimetric evaluation

Dosimetric comparison of CT and MRCAT plans was performed via cumulative dose-volume histograms (DVHs). This approach provides easy evaluation of dose coverage in key DVH points. Optimization criteria can be also easily checked.

DVH points evaluated in this study were chosen with respect to dose-volume criteria in our department (see Table 1) and those published by Korsholm.¹⁴

Difference between CT and MRCAT values in selected DVH points were represented by the following formula:

$$\Delta_{MRI} = \left| \frac{(MRCAT - CT)}{CT} \right|$$

where MRCAT stands for value in DVH point for MRCAT-based dose distribution, likewise the CT data. Thus, we obtain a relative difference between the CT and MRCAT plan with respect to the CT plan (in absolute values). The same procedure was applied to WE-based dose distribution:

$$\Delta_{WE} = \left| \frac{(WE - CT)}{CT} \right|$$

where WE stands for water equivalent, i.e. each voxel of MRCAT image was assigned a value of 0HU. Note that WE images do not contain anatomical information (except body contour), so CT and WE images cannot be registered directly. The registration parameters for WE dataset are identical to those of the MRCAT images from which the WE images were generated. It follows that Δ_{MRI} and Δ_{WE} are burdened by the same registration error.

Results were tested by statistical tests (significance level $\alpha=0.05$). First, normality of the data was tested. Then, one-sample t-test for Δ_{MRI} was performed. Δ_{MRI} and Δ_{WE} were compared by paired two-sample t-test.

As a supplement to our results, we carried out 2D gamma analyses of dose differences (CT to MRCAT and CT to WE) in a transversal plane crossing the isocenter. Region of 10 cm \times 10 cm surrounding the prostate was chosen for evaluation, and points in which $D < 5\% D_{max}$ were excluded.

Table 2 – Statistical results of the DVH points analysis. Δ_{MR} , Δ_{WE} refer to relative difference between MRCAT (or WE) with respect to CT. NS = non-significant.

		$\Delta_{\text{MR}} [\%]$ Mean \pm st.d.	$\Delta_{\text{WE}} [\%]$ Mean \pm st.d.	$\mu(\Delta_{\text{MR}}) \neq 0$ p-Value	$\Delta_{\text{MR}} < \Delta_{\text{WE}}$ p-Value
PTV2	$D_{2\%}$	0.5 ± 0.4	1.1 ± 0.6	0.008	<0.001
	$D_{50\%}$	0.5 ± 0.4	1.1 ± 0.5	0.00	<0.001
	$D_{95\%}$	0.6 ± 0.4	1.1 ± 0.7	<0.001	0.005
	$D_{98\%}$	0.7 ± 0.6	1.2 ± 0.9	0.004	0.006
	D_{max}	0.8 ± 0.7	1.4 ± 0.8	0.005	0.003
PTV1–2	$D_{95\%}$	0.8 ± 0.7	1.2 ± 0.9	0.001	0.005
	D_{max}	3.2 ± 8.1	3.5 ± 8.4	NS	NS
Rectum	$D_{10\%}$	0.9 ± 0.7	1.0 ± 0.7	0.04	NS
	$D_{30\%}$	0.6 ± 0.7	3.0 ± 5.2	0.021	NS
	$D_{60\%}$	0.6 ± 0.6	0.7 ± 0.5	0.011	NS
	$V_{75\text{Gy}}$	12.1 ± 10.7	22.9 ± 20.6	0.006	0.02
	$V_{70\text{Gy}}$	7.5 ± 6.3	9.2 ± 6.7	0.005	NS
	$V_{65\text{Gy}}$	3.5 ± 3.3	4.2 ± 3.2	0.007	NS
	$V_{60\text{Gy}}$	6.1 ± 13.2	6.5 ± 13.1	NS	NS
	$V_{50\text{Gy}}$	1.4 ± 1.3	1.4 ± 1.5	0.008	NS
	$V_{78\text{Gy}}$	77.6 ± 116.0	195.0 ± 333.0	NS	NS
Bladder	$V_{70\text{Gy}}$	3.7 ± 2.3	6.1 ± 3.2	0.001	<0.001
	$V_{60\text{Gy}}$	3.1 ± 2.4	4.1 ± 3.1	0.003	0.005
	$V_{50\text{Gy}}$	4.0 ± 6.2	4.6 ± 6.5	NS	0.005
	$D_{\text{max}} (\text{total})$	0.8 ± 0.7	1.4 ± 0.8	0.005	0.003
D_{mean} for PTV2		0.5 ± 0.4	1.1 ± 0.6	0.002	<0.001

Acceptance criteria for the test were 1%/1 mm. Results for MRCAT and WE were compared by paired two-sample t-test at the significance level $\alpha = 0.05$.

4. Results

Data for key DVH points are shown in Table 2. Table displays results of statistical test described above and values of Δ presented as mean \pm standard deviation.

Differences in almost all points $D_{X\%}$ did not exceed 2%. Only D_{max} for PTV1–2 was significantly higher because for one of the patients $D_{\text{max}} = 26\%$ which, regarding the number of patients, significantly influenced the mean value. Deviations in $V_{Y\text{Gy}}$ are noticeably higher, especially for high dose values. These results can be explained as follows: $V_{Y\text{Gy}}$ are in order of a few cm^3 , therefore only a slight deviation in the absolute number results in a considerable relative difference. To evaluate

these points, another method would be more suitable. Generally, values of Δ_{WE} are higher than those of Δ_{MRI} , which speaks to the benefit of the MRCAT provider.

Maps of gamma indexes for one patient are in Fig. 2 and general results are in Table 3. Mean pass rates are 93.4% for MRCAT plans and 82.5% for WE plans. Comparing MRCAT to WE (both for gamma and gamma pass rates), MRCAT was proven better than WE at the significance level $\alpha = 0.05$.

MRCAT or sCT planning receive an increasing attention and many studies have been published on this topic. Johnstone presented a review⁶ in which results of mentioned authors mostly did not exceed 2% of relative difference between CT and sCT dose distributions. Korsholm¹⁴ accepted 2% deviation in PTV coverage for 95% of the patients. This suggestion seems reasonable regarding errors such as registration error, interscan differences between two sessions, etc.¹ We reached reconcilable results, deviations in established DVH points did not exceed 2%. As for MRCAT, dose distributions, gamma pass

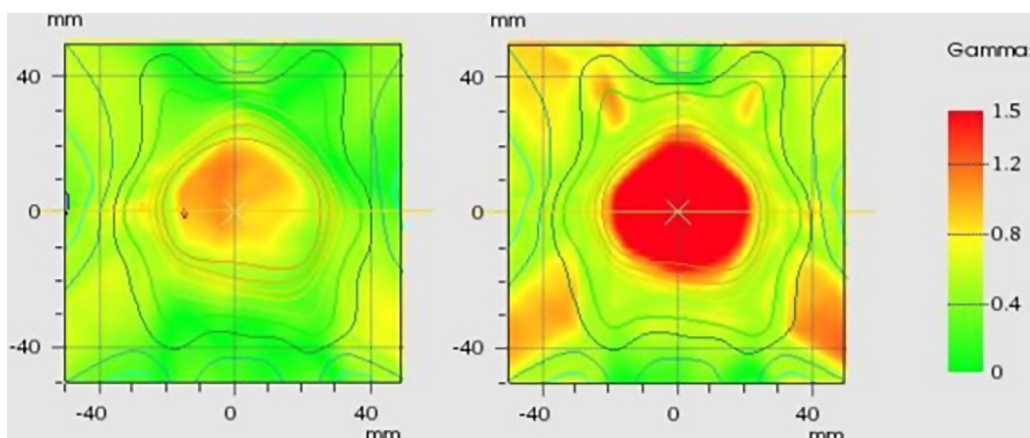


Fig. 2 – Maps of gamma indexes for one of the patients. Map assessing gamma values for MRCAT plan compared to CT plan is on the left, WE plan compared to CT plan is represented on the right.

Table 3 – Results of 2D gamma analysis for each patient. Acceptance criteria were set to 1%/1 mm. H* represents alternative hypothesis for paired two-sample t-test.

Patient	Mean gamma		Gamma pass rate [%]	
	MRCAT	0 HU	MRCAT	0 HU
A	0.45	0.75	97.5	83.8
B	0.81	1.12	69.9	50.4
C	0.46	0.53	98.1	96.0
D	0.38	0.45	100.0	99.1
E	0.45	0.63	98.8	88.9
F	0.32	0.48	98.5	94.3
G	0.33	0.68	100.0	79.4
H	0.32	0.56	100.0	93.1
I	0.65	0.75	87.3	75.9
J	0.66	0.89	83.4	64.0
H*	MRCAT < 0 HU		MRCAT > 0 HU	
p-Value	<0.001		<0.001	

rates exceeded 95% for 70% of the patients. Comparison of various authors is quite difficult though since they vary across the applied methods.

This study can be further enriched by other results. We suggest to perform plan optimization on MRCAT data and then transfer the plan to CT, alternatively to choose another image registration method.¹³ A larger patient cohort would also be suitable.

Putting MRCAT into practise leads to some changes in the standard workflow. The provider (Philips) offers simplified workflow, as presented by Köhler et al.¹⁰ Complete description of MRCAT implementation was published by Tyagi et al.¹⁵ From the perspective of our workplace, there are some shortcomings concerning MRCAT. MRCAT is tailored for image guidance based on DRR match or fiducial match. Nevertheless, cone-beam CT (CBCT) was adopted for treatment localization because small calcifications and other inhomogeneities can be used for matching the reference image and CBCT. These inhomogeneities are not clearly recognizable at MRCAT source images; thus, it cannot be considered as a reference image. For the same reason, the use of fiducial markers is problematic.

However, the above-mentioned problem is a matter of choosing a particular procedure that is incompatible with the MRCAT. A more significant problem is the limitations arising from the nature of MRI and MRCAT. The most important of these were ferromagnetic objects in the patient's body, especially in the field of view (causing errors in the resulting image), implanted pacemaker or atypical anatomy which the MRCAT algorithm cannot handle properly.¹⁶

5. Conclusions

In this study, no crucial difference between MRCAT and CT plans was demonstrated for clinically relevant DVH points. However, prior to MRCAT implementation, more in-depth analysis for a larger patient cohort is needed.

Conflict of interest

None declared.

Financial disclosure

None declared.

REFERENCES

1. Maspero M, Seevinck PR, Schubert G, et al. Quantification of confounding factors in MRI-based dose calculations as applied to prostate IMRT. *Phys Med Biol* 2017;62(3):948–66.
2. Roberson PL, McLaughlin PW, Narayana V, Troyer S, Hixson GV, Kessler ML. Use and uncertainties of mutual information for computed tomography/magnetic resonance (CT/MR) registration post permanent implant of the prostate. *Med Phys* 2015;32(2):473–82.
3. Devic S. MRI simulation for radiotherapy treatment planning. *Med Phys* 2012;39(11):6701–11.
4. Westbrook C, Roth CK. *MRI in practice*. John Wiley & Sons; 2011.
5. Dowling JA, Sun J, Pichler P, et al. Automatic substitute computed tomography generation and contouring for magnetic resonance imaging (MRI)-alone external beam radiation therapy from standard MRI sequences. *Int J Radiat Oncol Biol Phys* 2015;93(5):1144–53.
6. Johnstone E, Wyatt JJ, Henry AM, et al. A systematic review of synthetic CT generation methodologies for use in MRI-only radiotherapy. *Int J Radiat Oncol Biol Phys* 2017;100(1):199–217.
7. Edmund JM, Nyholm T. A review of substitute CT generation for MRI-only radiation therapy. *Radiat Oncol* 2017;12(1):28.
8. Han X. MR-based synthetic CT generation using a deep convolutional neural network method. *Med Phys* 2017;44(4):1408–19.
9. Kemppainen R, Suijamo S, Tuokkola T, et al. Magnetic resonance-only simulation and dose calculation in external beam radiation therapy: a feasibility study for pelvic cancers. *Acta Oncol* 2017;56(6):792–8.
10. Köhler M, Vaara T, van Grootel M, Hoogeveen R, Kemppainen R, Renisch S. MR-only simulation for radiotherapy planning – Whitepaper: Philips MRCAT for prostate dose calculations using only MRI data. *Philips White Paper* 2015.
11. Schubert G, Vaara T, Lindstrom M, Kemppainen R, van Grootel-Renses M. Commissioning of MR-only simulation for radiotherapy planning. *Philips White Paper* 2017.
12. Ghilezan MJ, Jaffray DA, Siewerdsen JH, et al. Prostate gland motion assessed with cine-magnetic resonance imaging (cine-MRI). *Int J Radiat Oncol Biol Phys* 2005;62(2):406–17.

13. Czajkowski P, Piotrowski T. Registration methods in radiotherapy. *Rep Pract Oncol Radiother* 2019;24:28–34.
14. Korsholm ME, Waring LW, Edmund JM. A criterion for the reliable use of MRI-only radiotherapy. *Radiat Oncol* 2014;9(1):16.
15. Tyagi N, Fontenla S, Zhang J, et al. Dosimetric and workflow evaluation of first commercial synthetic CT software for clinical use in pelvis. *Phys Med Biol* 2017;62(8):2961.
16. Christiansen RL, Jensen HR, Brink C. Magnetic resonance only workflow and validation of dose calculations for radiotherapy of prostate cancer. *Acta Oncol* 2017;56(6):787–91.